Vapor Pressure of Aluminum Chloride Systems. 1. Vapor Pressure and Triple Point of Pure Aluminum Chloride

John T. Viola, David W. Seegmiller, Armand A. Fannin, Jr., and Lowell A. King*
Frank J. Seiler Research Laboratory (Air Force Systems Command) and Department of Chemistry and Biological Sciences, United States Air Force Academy, Colorado 80840

The vapor pressures of solid and liquid pure aluminum chloride were measured from 114 to 256 °C. Samples were contained in Pyrex isoteniscopes which utilized mercury as the manometric fluid. The mercury columns were brought to null by an external pressure which was in turn measured at each experimental point. The triple point was determined from the intersection of the two vapor pressure–temperature curves. This value corresponded to 193.71 ± 0.03 °C and 1760 ± 1 Torr.

As part of an investigation of certain low-melting molten salt electrolytes for high energy density batteries, we needed to know the vapor density and vapor pressure of aluminum chloride. The former we have reported earlier (*13, 16*). Vapor pressures previously reported (*4, 5, 7, 9, 14, 15, 18, 19*) are at some variance, and we were uncertain which values to take. In some cases, they were not in a temperature range of interest to our work.

Experimental Section

Crystals of aluminum chloride which were prepared in a manner we have described previously (*17*) were loaded into Pyrex isoteniscopes such as shown in Figure 1. This operation was carried out in a glovebox with an atmosphere of nitrogen recirculated through a Linde (Trademark of Linde Division, Union Carbide Corp.) molecular sieve. The dew point was below −60 °C (less than 15 ppm H_2O). The valves were closed, and the isoteniscope was removed from the glovebox and assembled into the pressure measurement system. The system was evacuated and mercury introduced into the isoteniscope. It was then immersed in a well-stirred, thermostated oil bath. Bath temperatures were maintained and controlled with the aid of a platinum resistance element and Leeds and Northrup controller described elsewhere (*3*). Bath temperatures were measured to ±0.1 °C by determining the resistance of a nominal 100-Ω, four-wire platinum resistance element similar to the element used for control. The platinum resistors were calibrated against a platinum Air Force reference standard thermometer, which was calibrated at the freezing point of zinc, freezing point of tin, boiling point of water, triple point of water, and the boiling point of oxygen by the U.S. Air Force Measurement Standards Laboratory, Aerospace Guidance and Metrology Center, Newark Air Force Station, Ohio. In view of the extended immersion times between data collections and the absence of significant thermal gradients in the region of the bath occupied by the isoteniscope, we assumed the sample temperature to be the same as the bath temperature.

At each experimental temperature the mercury columns were brought to the same height as determined by a cathetometer by imposing an external pressure. The external pressures were measured in overlapping ranges with a McLeod gauge and a capacitance manometer (Type 210 Baratron Pressure Meter, MKS Instruments, Inc.). The two internal meniscus positions were measured to ±0.005 cm. Since two menisci were involved, a pressure uncertainty of ±0.1 Torr was ascribed to this measurement. The capacitance manometer was factory calibrated to yield a pressure uncertainty of ±0.02% of the measured pressure.

Pressure measurements were made at both ascending and descending temperature steps, and equilibrium was assured at each point by maintaining constant temperature for many minutes or, occasionally, hours, until pressure remained constant within measurement error. Five individual $AlCl_3$ samples were used. Special care was taken with one sample, with multiple measurements being taken over a 9-day period in the immediate vicinity of the triple point, with the bath temperature repeatedly being raised or lowered through the triple point temperature.

The data are shown in Table I. Pressures have been corrected for the vapor pressure of mercury within the isoteniscope. Interactions between Al_2Cl_6 vapor and Hg vapor were assumed to be negligible. The measurement method is indicated by a symbol after the pressure values. The symbols are defined in the table. The sample for which pressure was measured specifically in the vicinity of the triple point (as described above) is indicated by a "t" preceding the temperature value.

Results

We assumed vapor pressures of solid $AlCl_3$ and of liquid $AlCl_3$ could be represented by equations of the form

$$\log p = (A/T) + B \tag{1}$$

We chose to least-squares fit the data in such a way that uncertainties in both pressure and temperature could be taken into account. This was done by minimizing the perpendicular distance from the experimental point to the function given by eq 1. (Actually two such functions: one for the solid to vapor and one for the liquid to vapor.) This is the distance z in Figure 2. The minimum distance fitting technique, where the usual sharp distinction between independent and dependent variables is not necessary, is described in detail elsewhere (*6*). The perpendicular z does not quite reach the curve itself but contacts a chord drawn between the vertical and horizontal projections of the experimental point onto the curve. Obviously z can be either longer or shorter than the true perpendicular distance to the curve, depending upon which side of the curve the datum lies. In the case of the data taken specifically in the vicinity of the triple point (indicated by "t" on Table I), the root mean square value of the quantity $|(z - \text{true perpendicular})|/(\text{true perpendicular})$ was 0.000 002 and 0.000 004 for the solid and liquid phases, respectively. We solved for values of A and B which minimized the sum $\Sigma_{i=1}{}^{N} z_i{}^2$ where

$$z_i = \left[\frac{1}{\left(\frac{\delta p}{p_{\text{exp},i} - p_{\text{eqn},i}}\right)^2 + \left(\frac{\delta T}{T_{\text{exp},i} - T_{\text{eqn},i}}\right)^2} \right]^{1/2} \tag{2}$$

Table I. Experimental Data

t^a	p^b	t^a	p^b
	Solid to Vapor		
113.66	3.77 m	158.28	168.02
113.66	3.80	163.40	230.13
114.37	3.92 m	163.40	230.63
116.70	5.52	163.40	235.66
116.70	5.53 m	169.90	376.17
118.50	6.30 m	176.80	573.20
118.50	6.32	176.80	574.97
119.37	7.14 m	179.49	716.93
119.37	7.25	t 179.66	696.79
122.87	9.36 m	t 181.84	808.52
124.23	10.91 m	t 184.00	934.15
124.23	10.94	t 184.08	943.10
125.61	10.80 m	t 184.08	952.31
127.97	15.09	t 186.25	1082.23
128.45	16.26 m	187.27	1157.09
128.45	16.36 m	t 187.87	1203.41
128.63	16.47	t 189.49	1344.23
130.92	19.03 m	t 190.49	1428.89
137.46	33.81	t 190.82	1461.56
140.42	41.13	t 191.44	1522.82
144.53	58.15	t 191.95	1567.17
149.66	88.42	t 192.63	1641.14
152.44	106.05	t 192.79	1660.37
152.49	103.78	t 193.17	1705.21
	Liquid to Vapor		
t 182.52	1389.69	220.97	3007.24
t 182.52	1391.82	221.03	3009.18
t 186.14	1499.91	223.30	3159.62
t 188.03	1562.36	226.14	3294.32
t 189.65	1615.69	226.14	3294.32
t 190.44	1642.33	226.20	3296.76
t 191.71	1686.27	226.25	3300.19
t 192.63	1719.79	226.25	3328.64
t 193.88	1766.41	226.30	3301.64
194.58	1757.10	226.39	3305.03
t 195.10	1809.01	226.44	3309.96
t 196.56	1864.93	228.88	3482.82
t 197.86	1915.67	231.51	3615.85
t 199.14	1967.38	231.56	3614.30
199.82	1936.82	231.62	3619.21
t 200.52	2024.01	231.62	3649.00
t 202.15	2092.44	231.73	3620.57
204.08	2235.00	231.78	3626.49
t 204.60	2191.60	231.81	3624.96
209.74	2481.71	231.84	3626.92
210.26	2472.36	235.68	3915.56
210.28	2471.34	236.72	3948.48
210.31	2473.32	236.75	3949.45
210.31	2473.32	236.77	3951.44
210.34	2474.29	236.80	3951.91
215.08	2706.13	236.88	3954.31
215.11	2707.10	236.91	3957.31
215.13	2708.08	236.94	3957.77
215.19	2708.53	236.97	3958.23
215.21	2709.51	236.97	3958.73
215.21	2711.01	236.99	3962.24
215.24	2721.97	239.03	4134.67
215.27	2711.46	239.05	4138.17
215.27	2711.96	242.68	4390.79
218.00	2882.75	245.57	4604.78
220.67	3018.51	248.19	4795.18
220.81	3001.40	250.94	5012.84
220.89	3003.83	251.00	5063.27
220.89	3003.83	253.64	5270.21
220.97	3006.74	256.52	5511.66

[a] The symbol "t" indicates the sample for which the triple point was determined. [b] The symbol "m" indicates the use of a McLeod gauge for pressure measurement; all other measurements were made with a capacitance manometer.

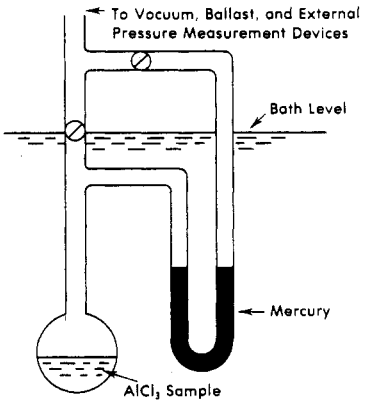

Figure 1. Isoteniscope.

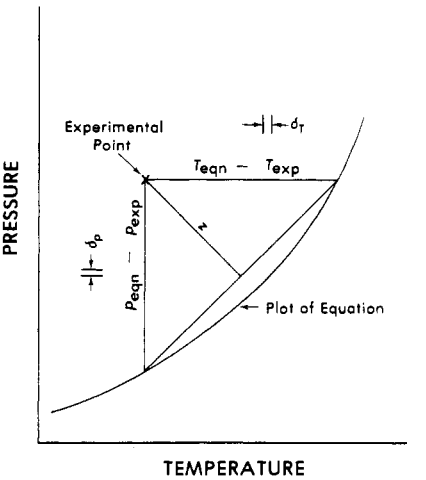

Figure 2. Least-squares fitting scheme.

Table II. Equations to Determine $AlCl_3$ Triple Point

For Solid to Vapor (179.7–193.2 °C)
$\log p = -(6029.5925/T) + 16.160681$
$s_p = 0.004$ Torr, $s_T = 0.06°$

For Liquid to Vapor (182.5–204.6 °C)
$\log p = -(1956.530/T) + 7.436296$
$s_p = 0.02$ Torr, $s_T = 0.05°$

Equation 2 is derived elsewhere (*6*). In eq 2, $p_{eqn,i} = \exp[(A/T_{exp,i} + B) \ln (10)]$ and $T_{eqn,i} = A/[\log (p_{exp,i}) - B]$. Table I lists $p_{exp,i}$ and $t_{exp,i}$ (from which $T_{exp,i}$ can be obtained). These least-squares fits were iterative. Iterations were continued until

$$\frac{2|(\sigma - \sigma_{\text{previous iteration}})|}{\sigma + \sigma_{\text{previous iteration}}} < 10^{-7} \quad (3)$$

where σ, the standard deviation, was calculated from

$$\sigma = \left[\frac{1}{N}\sum_{i=1}^{N} z_i^2\right]^{1/2} \quad (4)$$

The values of A and B for the equations in Table II are those obtained when the criterion of eq 3 was first satisfied.

The solid to vapor and liquid to vapor lines intersect at T = 466.86 K and p = 1759.8 Torr. Confidence hyperbolas were calculated (*1*) for each line in order to establish the uncertainty in the intersection values of T and p. Such hyperbolas allow one to take into account the interdependency of A and B in fitting to real data. The hyperbolas were constructed assigning all of the error along the $1/T$ axis. This led to 95% confidence limits of ±0.03 K and ±0.06 K for the liquid to vapor and solid to vapor

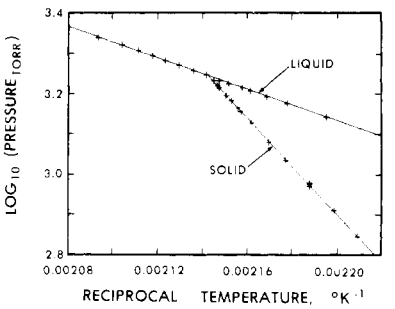

Figure 3. Vapor pressure data near the triple point: +, experimental points; —, equations from Table II.

Table III. Equations for the Vapor Pressure of $AlCl_3$

For Solid to Vapor (113.7–193.2 °C)
$\log p = -(5900.71/T) + 15.88462$
$s_p = 0.2$ Torr, $s_T = 0.2°$

For Liquid to Vapor (182.5–256.5 °C)
$\log p = -(1956.06/T) + 7.43530$
$s_p = 0.3$ Torr, $s_T = 0.4°$

lines, respectively. These in turn correspond to ±1.0 and ±7.2 Torr for the liquid to vapor and solid to vapor lines, respectively.

Since the intersection values must satisfy the solid to vapor and the liquid to vapor data, we report the lesser of the uncertainties, viz., the triple point is 466.86 ± 0.03 K and 1760 ± 1 Torr.

If the triple point is considered fixed, eq 1 becomes

$$\log p = A\left(\frac{1}{T} - \frac{1}{T_x}\right) + \log p_x \qquad (5)$$

We then least-squares fit all the data of Table I to two functions of the form of eq 2, where, from eq 5, $p_{eqn,i} = \exp\{[A(1/T_{exp,i} - 1/T_x) + \log(p_x)]\ln(10)\}$ and $T_{eqn,i} = A/\{\log(p_{exp,i}) - \log(p_x) + A/T_x\}$.

Iterations were performed until the criterion in eq 3 was satisfied.

The root mean square value of the quantity |(z − true perpendicular)|/(true perpendicular) was 0.003 and 0.000 03 for solid and for liquid phases, respectively.

The values of A for the equations in Table III are those obtained when the criterion of eq 3 was first satisfied. The values of B were calculated from $B = \log(1759.8) - A/466.86$.

The data used to determine the triple point and the equations given in Table II are illustrated in Figure 3. A plot of all data and the equations of Table III would appear very similar with essentially no more visible scatter than can be detected in Figure 3.

Discussion

The present liquid $AlCl_3$ vapor pressures agree within −1 to +1.5% with the pressures measured by Nisel'son et al. (*15*) and Smits and Meijering (*18*) over shorter temperature spans. The data of Fischer and Rahlfs (*7*) extend to much higher temperatures than we reached, and disagree by as much as 10% with our data at their lowest temperature, 194 °C.

Solid $AlCl_3$ always achieved a constant value of vapor pressure after a temperature change much more slowly than did liquid $AlCl_3$. In fact, we did not report any data for the solid phase until we had observed no detectable change in pressure for a 1-h period. Such slow attainment of equilibrium is typical of solid $AlCl_3$; every operation in our laboratory which entailed a phase change from or to the solid has been found to occur very slowly. This slow attainment of a constant vapor pressure was noted also by Fischer and Rahlfs (*7*) and Smits and Meijering (*18*), whose data agree with ours within less than 5% over shorter temperature spans.

Table IV. Enthalpy and Entropy of Phase Transformations

Compd	ΔH_{sl}, kcal mol^{-1}	T_{sl}, K	ΔS_{sl}, cal deg^{-1} mol^{-1}	ΔS_{lg}, cal deg^{-1} mol^{-1}	Ref
Al_2Cl_6	18.64	466.86	39.92	19.18[a]	Present work
Al_2Br_6	5.38	370.6	14.5	21.6	12
Al_2I_6	7.6	464.15	16		12
Fe_2Cl_6	20.60	577	35.7	20.3[b]	12

[a] At the triple point temperature, 466.86 K. $\Delta S_{lg} = 21$ cal deg^{-1} mol^{-1} at extrapolation of liquid to vapor curve to $p = 760$ Torr, i.e., 429 K. [b] Reference 20.

The data of Galitskii (*9*) and of Maier (*14*), who did not make note of any unusual behavior by solid $AlCl_3$, disagree markedly with ours, with differences ranging from −14 to +240%.

The peculiarities associated with melting and vaporization of solid $AlCl_3$ have been examined in some detail (*8, 18*), but so far no definite explanations of the behavior have been established. While the chloride, bromide, and iodide of aluminum all are dimeric (i.e., Al_2X_6) in the liquid and vapor states, only the latter two are reported to have the same molecular structure as solids, whereas the chloride exhibits a layered, approximately close-packed chloride ion structure similar to that of $CrCl_3$ and $FeCl_3$ (*2, 10, 11, 18*). We have previously noted the obviously layered structure of $AlCl_3$ crystals (*17*).

Comparison is made in Table IV of the enthalpy and entropy of phase transformations of $AlCl_3$ with various other substances.

The compressibility factor can be calculated from the saturated vapor pressure and vapor density (*13*) from eq 6

$$Z = 266.67p/dRT \qquad (6)$$

Z varies from 0.97 to 0.78 over the temperature range 188–254 °C, respectively, in nearly a linear manner.

Our data for both solid and liquid $AlCl_3$ vapor pressure show much less scatter than those of the other investigators (except the liquid data of Smits and Meijering (*18*) whose data precision is about the same as ours). Smits and Meijering (*18*) also report a triple point obtained from the intersection of the solid and the liquid vapor pressure curves. Their value, 192.6 °C at 1715 Torr, is slightly lower than ours.

Safety

Appropriate precautions should be taken for the containment of liquids above their normal boiling points in glass vessels. It is also important to consider that mercury has an appreciable vapor pressure at elevated temperatures (ca. 90 Torr at the highest temperature reached in the present study).

Glossary

A	fitted constant
B	fitted constant
d	vapor density
g	gas
i	index for individual points
l	liquid
ln	natural logarithm
log	logarithm to the base 10
N	the total number of experimental points used for a given least-squares fit
p	pressure, Torr
p_x	triple point pressure, Torr
s	solid

s_p	root mean square of differences between experimental pressure and pressure at the corresponding intersection of the perpendicular to the chord
s_T	root mean square of the difference between experimental temperature and temperature at the corresponding intersection of the perpendicular to the chord
t	temperature, °C
T	temperature, K
T_{mn}	temperature of transition from state m to state n, K
T_x	triple point temperature, K
z	perpendicular distance to chord along equation; function to be treated by least-squares fitting
Z	compressibility factor
δp	the greater of 0.1 Torr or 0.0002 p; estimated uncertainty in pressure measurement
δT	0.1 K; estimated uncertainty in temperature of apparatus
ΔH_{mn}	enthalpy change from state m to state n, kcal mol^{-1}
ΔS_{mn}	entropy change from state m to state n, cal deg^{-1} mol^{-1}
σ	standard deviation

Literature Cited

(1) Acton, F. S., "Analysis of Straight-Line Data", Dover, New York, N.Y., 1966, pp 14–34.
(2) Bigelow, M. J., *J. Chem. Educ.*, **46**, 495 (1969).
(3) Brabson, G. D., Fannin, Jr., A. A., *Rev. Sci. Instrum.*, **44**, 338 (1973).
(4) Denisova, N. D., Baskova, A. P., *Russ. J. Phys. Chem.*, **43**, 1317 (1969).
(5) Dunne, T. G., Gregory, N. W., *J. Am. Chem. Soc.*, **80**, 1526 (1958).
(6) Fannin, Jr., A. A., King, L. A., Frank J. Seiler Research Laboratory Technical Report, SRL-TR-76-19 (1976).
(7) Fischer, W., Rahlfs, O., *Z. Anorg. Allg. Chem.*, **205**, 1 (1932).
(8) Foster, L. M., *J. Am. Chem. Soc.*, **72**, 1902 (1950).
(9) Galitskii, N. V., *Russ. J. Inorg. Chem.*, **13**, 1607 (1968).
(10) Gerding, H., Smit, E., *Z. Phys. Chem., Abt. B*, **50**, 171 (1941).
(11) Harris, R. L., Wood, R. E., Ritter, H. L., *J. Am. Chem. Soc.*, **73**, 3151 (1951).
(12) "JANAF Thermochemical Tables", Dow Chemical Co., Midland, Mich., 1974.
(13) King, L. A., Seegmiller, D. W., *J. Chem. Eng. Data*, **16**, 23 (1971).
(14) Maier, C. G., Technical Paper 360, Department of the Interior, Bureau of Mines, 1925.
(15) Nisel'son, L. A., Pustil'nik, A. I., Gavrilov, O. R., Rodin, V. A., *Russ. J. Inorg. Chem.*, **10**, 1271 (1965).
(16) Seegmiller, D. W., Fannin, Jr., A. A., Olson, D. S., King, L. A., *J. Chem. Eng. Data*, **17**, 295 (1972).
(17) Seegmiller, D. W., Rhodes, G. W., King, L. A., *Inorg. Nucl. Chem. Lett.*, **6**, 885 (1970).
(18) Smits, A., Meijering, J. L., *Z. Phys. Chem., Abt B*, **41**, 98 (1938).
(19) Stull, D. R., *Ind. Eng. Chem.*, **39**, 540 (1947).
(20) Todd, S. S., Coughlin, J. P., *J. Am. Chem. Soc.*, **73**, 4184 (1951).

Received for review April 5, 1976. Resubmitted March 8, 1977. Accepted May 7, 1977.

Standard Potential of the Mercury–Mercurous Benzoate Electrode at 20 °C

Thomas P. Russell and John F. Reardon*
Chemistry Department, Boston State College, Boston, Massachusetts 02115

The standard potential of the mercury–mercurous benzoate electrode has been determined to be 430.64 ± 0.09 mV in aqueous benzoic acid solutions at 20 °C. The standard potential between 20 and 40 °C is given to within ±0.1 mV by the expression $E^\circ = 0.4480 - (945.7 \times 10^{-6})t + (3.429 \times 10^{-6})t^2$.

Mercury–mercurous carboxylate electrodes have aroused considerable interest recently as possible internal reference electrodes for ion-selective electrodes (*3*). As part of a systematic study of these carboxylate electrodes we report the results of our investigation of the mercury–mercurous benzoate electrode. This electrode had been investigated previously from 25 to 40 °C by Bertram and Bone (*1*) and at 25 °C by Chauchard and Gauthier (*2*). In these prior investigations classical paste electrodes had been used. In this study the skin-type electrode described by Hills and Ives (*4*) for the calomel electrode which led to the improvement in performance of that electrode was used.

Electromotive force measurements of the cell of the type $Pt|Q{\cdot}QH_2|HBz(m)|Hg_2Bz_2|Hg$ have been made at 20 °C. The acid concentrations ranged from 0.005 to 0.015 mol kg^{-1}. The standard potential was computed from a thermodynamic analysis of the data.

Experimental Section

Mercurous benzoate was prepared and stored as described by Bertram and Bone (*1*). Mercury was triple distilled and was purified by the method of Hills and Ives (*4*). Fisher reagent grade quinhydrone was recrystallized from conductivity water acidified with benzoic acid (pH 5) and stored in a desiccator over quinone in the dark. Baker Primary Standard benzoic acid was used as received. Benzoic acid solutions were made up volumetrically and weighed aliquots titrated with carbonate-free standardized sodium hydroxide. Oxygen was excluded during all preparations and procedures through the use of nitrogen.

The electrode cell compartments were similar to those used by Larson and MacDougall for the mercury–mercurous acetate electrodes (*7*) and were arranged similarly. The mercurous benzoate cells were rendered hydrophobic by treatment with Clay Adams wetting solution and the quinhydrone cells were painted black. Electrodes for the quinhydrone half-cells were of platinum wire (22 gauge) sealed in soft glass tubing (*9*).

The mercury–mercurous benzoate cell solution was prepared by stirring a deaerated benzoic acid solution, mercurous benzoate, and mercury for 72 h in the dark under nitrogen. The mercurous benzoate skin was prepared by shaking mercury and mercurous benzoate in a small flask and adding both mercury and skin to a clean mercury surface in the cell compartment. The previously stirred cell solution was added. Quinhydrone electrodes were prepared by adding quinhydrone twice washed with cell solution to deaerated benzoic acid. Three electrodes of each type which agreed to 0.05 mV were made for each run and three runs were made for each concentration. The thermostat was a transformer oil bath. Temperature control was to 0.02 °C and the temperature was verified with an NBS calibrated thermometer.